DOI: 10.1002/asia.200900713

Hybridization of Long Pyridine-Dicarboxamide Oligomers into Multi-Turn Double Helices: Slow Strand Association and Dissociation, Solvent Dependence, and Solid State Structures

Benoit Baptiste,[b] Jiang Zhu,[a] Debasish Haldar,[a] Brice Kauffmann,[a] Jean-Michel Léger,[b] and Ivan Huc*[a]

Abstract: Oligoamides of 2,6-diaminopyridine and 2,6-pyridinedicarboxylic acid comprised of 5, 7, 9, 11, or 13 units and bearing 4-isobutoxychains on all pyridine rings and *tert*-butyl-carbamate terminal groups have been synthesized stepwise, along with an 11 mer having benzyl-carbamate terminal groups. The crystal structure of all five Boc-terminated compounds has been obtained and shows a highly regular and conserved double helical hybridization motif of up to 3 complete turns for the 13 mer. Four pyridine units span one helical turn and define a helix pitch of *ca* 7 Å. Solution studies in $CDCl_3$ demonstrated that the Boc-terminated oligomers strongly hybridize in this solvent, and that K_{dim} values increase with oligomer length. The K_{dim} values are 31000 and 7×10^5 L mol^{-1} for the 7 mer and the 9 mer, respectively, and are too high to be measured by NMR for the 11 mer and the 13 mer. Hybridization and dissociation kinetics at 2 mM proceed at decreasing rates upon increasing oligomer length. The rate was faster than minutes for the 7 mer, of the order of hours for the 9 mer, and days for the 11 mer and 13 mer. The same trend was observed in [D_5]pyridine but with considerably lower K_{dim} values and faster kinetics. The benzylcarbamate 11 mer was also found to hybridize into a double helix but with reduced K_{dim} values and faster kinetics compared to its Boc-terminated analogue. Combined with previous studies, the results presented here frame a global understanding of the hybridization of these pyridinecarboxamide oligomers and provide useful guidelines for the design of other artificial double helices.

Keywords: chirality · helical structures · structure elucidation · supramolecular chemistry · X-ray diffraction

Introduction

Nature has found very diverse applications of the hybridization of organic molecular strands into double or triple helical architectures. In nucleic acids, sequence selective hybridization is key to genetic information storage,[1] duplication, and transcription. In the triple helix of collagen,[2] some polysachharides[3] or in coiled coils (e.g., keratin[2a,4]) hybridization contributes to the stiffness and mechanical properties of the polymer fibers. In the bacterial peptide gramicidin D, hybridization gives rise to a double stranded β-helix architecture that can bind metal ions in its cavity.[5] Except in the case of short oligomers such as Gramicidin D, hybridization in biopolymers occurs over extended lengths which confers the hybrids with considerable thermodynamic and kinetic stability. Nevertheless, nucleic acid duplexes or collagen gels melt at high temperatures as a result of strand dissociation, which reveals a high negative entropy of hybridization.[1b]

[a] Dr. J. Zhu,[++] Dr. D. Haldar,[#] Dr. B. Kauffmann, Dr. I. Huc
Université de Bordeaux—CNRS UMR 5248 and UMS 3033
Institut Européen de Chimie et Biologie
2 rue Robert Escarpit, 33067 Pessac (France)
Fax: (+33) 540-002-215
E-mail: i.huc@iecb.u-bordeaux.fr

[b] B. Baptiste,[+] J.-M. Léger
Université Victor Ségalen Bordeaux 2
EA 4138 - Pharmacochimie
146 rue Léo Saignat, 33076 Bordeaux Cedex (France)

[++] Present address:
Division of Chemistry, North Sichuan Medical College
234 Fujiang Lu, Nanchong 637007 (China)

[#] Present address:
Department of Chemical Sciences
Indian Institute of Science Education and Research, Kolkata.
Haringhata, Mohanpur, West Bengal 741252 (India)

[+] These authors contributed equally to this work

Supporting information for this article is available on the WWW under http://dx.doi.org/10.1002/asia.200900713.

Strand association in those cases is thus a highly cooperative process.

Inspired by the remarkable efficiency of biopolymer hybridization, chemists have synthesized a number of non-natural molecular strands that also possess the ability to intertwine into multiple helices.[6] Prominent examples include metal coordination-based helicates,[7] a plethora of nucleic acid analogues,[8] aromatic oligoamides,[9] D,L-peptides inspired from gramicidin D,[10] oligo-resorcinols,[11] ethynylhelicene oligomers,[12] *m*-terphenyl backbone oligomers exploiting amidinium-carboxylate salt bridges,[13] alternate sequences of aromatic hydrogen-bond donors and acceptors,[14] or some mannose-derived δ-peptides.[15] Mention should also be made of sheet-like structures in which hybridization occurs without helical winding.[16,17] These synthetic model systems allow the exploration of hybridization patterns which differ from those in Nature and thus shed light on the essential features of biopolymers that govern their hybridization behavior. Indeed, the thermodynamic and kinetic behaviors of several synthetic duplex families apparently differ significantly from those of their natural counterparts. The thermodynamic stability of non natural hybrids was shown in several cases to level off or even drop upon strand length increase.[9c,11d,17] Kinetic stability may reach very high levels, which allows the chromatographic separation of artificial duplexes from single strands or other duplexes despite the small size of these non-covalent assemblies.[9j,l,12c] Additionally, hybridization mechanisms other than a simple zipper-like process have been proposed. For example, molecular modeling studies hinted at a slippage mechanism that involves a series of roller-coaster-like discrete steps[18] in which the intramolecular interactions within a single helix are replaced by intermolecular interactions in the duplex when the tail of one of the strands proceeds inside the other single helix in an eddy-like process. Such mechanisms may eventually allow direct strand exchange between two duplexes without dissociation[11d] and the involvement of pre-equilibration with structural intermediates prior to reaching thermodynamic equilibrium.[12c]

These intriguing results concern different artificial duplex families and obviously call for further physical and structural investigations of the hybridization processes. In particular, because of the lack of accessibility of well defined oligomers longer than just a few units, previous studies have generally focused on helices spanning only one or two turns and data concerning longer sequences are scarce (for notable exceptions, see references [9c, 11d, and 12c]). In the case of pyridine oligoamides, we have initially reported the unexpected trend that double stranded hybrid stability tends to drop when oligomer length increases.[9c] We have also shown that short sequences (5 to 9 monomers) are able to form several types of duplex architectures in which the two strands may be offset by zero,[9d] one,[9b,k] or two[9a,f] monomers, consistent with the dynamics observed in solution[9a] and with calculations.[18] Recently, we demonstrated that hybridization is a mostly enthalpically driven process in which the high cost of spring-like extension of single helical monomers observed during hybridization is compensated by the large enthalpy gain that results from interstrand π–π stacking in the duplex.[9i] The study reported here aimed at a thorough structural investigation of the double helices of long pyridine oligoamides sequences. It was carried out in order to explore whether structural variability as observed for shorter sequences persist with more than nine units, and also with the hope that structural insights would help elucidate the trend of affinity versus strand length. As shown in the following, we found compelling crystallographic evidence that hybridization of pyridinecarboxamide oligomers may occur over extended lengths. Additionally, solution-phase investigations of the newly synthesized oligomers allowed us to characterize the high solvent dependence of the hybridization process and the dramatic effect of strand length on the association and dissociation kinetics which span several orders of magnitude upon adding a few units. In turn, the observation of slow hybridization kinetics for longer oligomers led us to re-investigate the association constants and to revise our initial proposal that hybridization drops upon strand length increase. Indeed, we now unambiguously show that duplex stability considerably *increases* upon strand length increase. Finally, we show that bulky terminal Boc groups favor hybridization thermodynamics and slow down hybridization kinetics. Both these findings have implications regarding the hybridization mechanism.

Results and Discussion

Molecular Design

In previous studies, the long pyridinecarboxamide oligomers investigated were equipped with *n*-decyloxy side chains which provide excellent solubility in organic solvents but prevent the growth of high quality single crystals for solid-state structural investigations. In the meantime, studies of related single helical quinoline carboxamide oligomers showed that isobutoxy side chains provide both high solubility in chlorinated and aromatic solvents, and high crystallinity,[19] even for very large oligomers.[20] We thus decided to undertake the synthesis of pyridinecarboxamide oligomers **5a**–**13a**, possessing from 5 to 13 units and having isobutoxy side chains in position 4 of each pyridine ring. These substituents diverge from the helices and are exposed to the solvent. They also strongly influence the hybridization process: oligomers that carry alkoxy groups on every residue hybridize into double helices possess K_{dim} values that are several orders of magnitude larger than oligomers with no such substituents.[9a,b] However, it was also shown that the

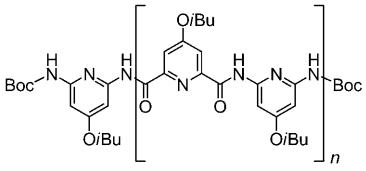

n = 2: **5a**
n = 3: **7a**
n = 4: **9a**
n = 5: **11a**
n = 6: **13a**

effect of alkoxy residues on hybridization does not depend on the nature of the alkyl group, and so *n*-decyloxychains have the same effect as methoxy groups.[9k] It was thus assumed that isobutoxy groups would result in a similar propensity towards hybridization.

Synthesis

Thanks to the experience acquired in the stepwise preparation of various families of long arylamide oligomers, we opted for a divergent approach different from that previously used in oligopyridine-dicarboxamide synthesis, and made use of the efficient activation of carboxylic acids as acid chlorides under neutral conditions with 1-chloro-*N*,*N*,2-trimethylpropenylamine[21] in the presence of Boc amine protection. This allowed us to avoid benzylcarbamate protection (Cbz) which, in our experience, sometimes proved to be difficult to remove from large folded oligomers. The synthetic schemes were designed taking into account that helical folding creates a severe steric hindrance,[19b,22] and our observation that this is particularly acute if reagents also undergo hybridization into stable double helices. Thus, our choice was to attach "small" units that do not hybridize (dimer acid chlorides) at the ends of longer diamine oligomers. Much higher yields were observed upon coupling a small acid chloride to a large diamine than coupling a small amine to a large diacid chloride. Thus, the synthesis proceeded through the early desymmetrization of diester **1a** into monoacid **1b** and of diamine **1d** into monoamine **1e** (Scheme 1). Coupling between **1e** and **1d** afforded the key intermediate dimer **2a**, which was saponified to give **2b**. After activation as an acid chloride, **2b** was used repeatedly to elongate the diamine precursors by four pyridine units (Scheme 2). Thus, diamine monomer **1b** was elongated to pentamer **5a**, which after Boc deprotection, was converted to nonamer **9a**. One more deprotection/coupling round led to tridecamer **13a**. Similarly trimer **3a** was converted to heptamer **7a** and then to the undecamer **11a**.

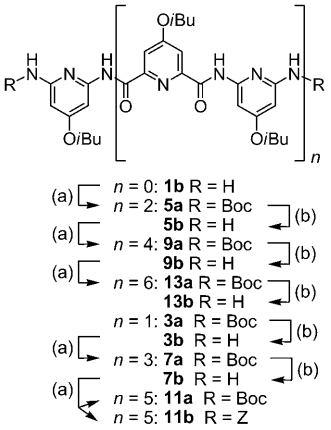

Scheme 2. a) **2b** or **2d**, 1-chloro-*N*,*N*,2-trimethylpropenylamine, CH_2Cl_2, then DIEA, CH_2Cl_2; b) TFA, CH_2Cl_2.

Solid-State Characterization

As anticipated, the isobutoxy group in position 4 of the pyridine rings conferred the oligomers with high solubility in chlorinated and aromatic solvents and with a remarkable propensity to crystallize. Single crystals of the five compounds, namely **5a**, **7a**, **9a**, **11a**, and **13a**, suitable for X-ray diffraction analysis were all obtained upon diffusion of MeOH into a $CHCl_3$ solution of the compounds. Alternatively, the same crystals could be obtained upon slow evaporation of a methanol–chloroform solution of the compounds. In some cases, centimeter long crystals grew in a few days. All structures were solved using ab initio methods despite the large asymmetric units of some of them and all revealed a double helical architecture (Figure 1).

The crystallographic parameters are reported in Table 1. We have found that the level of crystallographic symmetry increases with oligomer length. The 5 mer and 7 mer crystallized in the $P\bar{1}$ space group with two double helices in the asymmetric unit whereas the 9 mer and the 11 mer were obtained in the $P\bar{1}$ and *Pbca* space groups, respectively, with only one double helix in the asymmetric unit. The 13 mer was solved in the monoclinic *C*2/*c* group and, in this case, the two strands of the duplex are related by a crystallographic C_2 axis and the asymmetric unit is reduced to one strand.

The hybridization motifs of **5a**–**13a** are strictly identical. Each strand of the duplex spans one helical turn every four pyridine units for a vertical rise per turn of 7 Å. Direct contacts between the two strands consist essentially of face-to-face aromatic stacking. The two strands of each duplex are helically

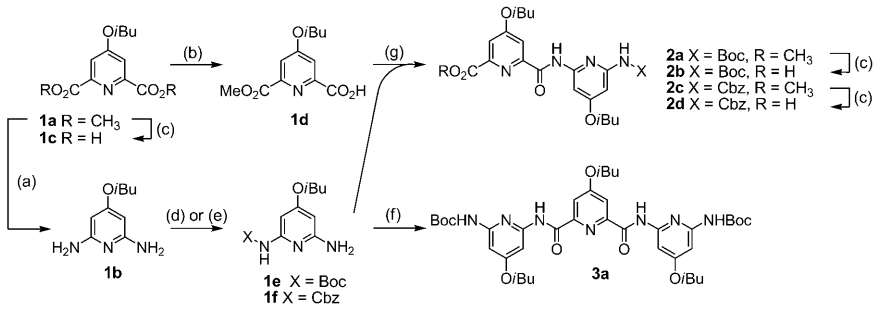

Scheme 1. a) *1*- NH_3 gas, MeOH, 1 h, RT; *2*- KOH, Br_2, dioxane, 0 °C for 10 min then 25 °C for 30 min and 70 °C for 1.5 h, 78% yield; b) NaOH, MeOH/dioxane, 2 h, 25 °C, 72% yield; c) NaOH, MeOH/dioxane/water, 2 h, RT, 95% yield; d) lithium bis(trimethylsilyl)amide, di*tert*-butyldicarbonate, THF, 3.5 h, RT, 52% yield; e) lithium bis(trimethylsilyl)amide, benzyl chloroformate, THF, 3.5 h, RT, 56% yield; f) *1*- **1c**, $SOCl_2$, 30 min, reflux; *2*- **1e**, DIEA, THF ; 12 h., 25 °C, 75% yield; g) *1*- **1d**, $SOCl_2$, 30 min, reflux *2*- **1e**, DIEA, THF, 12 h., 25 °C, 81% yield for **2a**; *1*- **1d**, oxalyl chloride, DMF, toluene, 2 h, RT; *2*- **1f**, DIEA, THF, 12 h, RT, 98% for **2c**.

CHEMISTRY
AN ASIAN JOURNAL

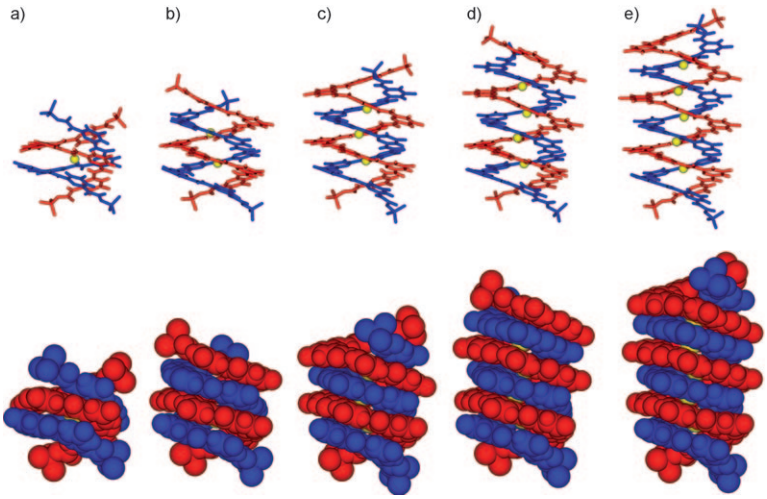

Figure 1. Side view of the solid-state structures in stick (top) and CPK (bottom) representations of: a) pentamer **5a**; b) heptamer **7a**; c) nonamer **9a**; d) undecamer **11a**; e) tridecamer **13a**. The two strands of the double helices are shown as red and blue and water molecules as yellow sticks. Isobutoxy side chains, hydrogen atoms and solvent molecules (except water included in the channel) have been omitted for clarity. All helices are displayed in the same orientation, as illustrated by the identical appearance of their lower part.

offset with respect to one another. This offset is constant for all duplexes, which is about one aromatic ring, that is, one quarter of a turn. Thus, ring 1 of strand A stacks over ring 2 of strand B, and reciprocally. The conservation of the hybridization motif is in contrast with previous observations that the two strands may adopt different relative positions within a duplex, which results in offsets of zero, one, or two pyridine units. These observations were made on shorter strands (5–9 units) and the highest variability was observed for pentameric oligomers. Thus, it appears that elongation of the strands reduces their relative mobility (i.e., screw-like motions) within the duplex and that a dominant structural pattern emerges for extended lengths. For the 13 mer, these features result in a 2.6 nm long duplex having a molecular weight above 5.3 kDa in which each strand spans over three helical turns. The regularity of the helical pattern, from the 5 mer to the 13 mer also suggests that it might be propagated along much longer (e.g., polymeric) sequences without any alteration of the interactions.

The polar cavity of the double helix channel is filled by water molecules, one for the pentamer, and an additional water molecule for every two additional pyridine units on each strand (Figure 1). Additionally, the extremities of the channel are closed by the OH group of a bound methanol molecule that occupies a position similar to those occupied by water (not shown). We notice here the high conservation of the position of water molecules throughout the series. Each water oxygen atom may potentially hydrogen bond to the four amide protons of the two pyridinecarboxamide units, one on each strand, oriented perpendicularly to each other (Figure 2). Other possible interactions involve hydrogen-bonding of the water hydrogen atoms to endocyclic nitrogens of the neighboring 2,6-diaminopyridine units

Table 1. Crystallographic parameters for **5a–13a**.

	5a	**7a**	**9a**	**11a**	**13a**
Solvent of cryst.	$CHCl_3$/MeOH	$CHCl_3$/MeOH	$CHCl_3$/MeOH	$CHCl_3$/MeOH	$CHCl_3$/MeOH
Formula	$C_{59}H_{79}N_{11}O_{13}$	$C_{79}H_{103}N_{15}O_{17}$	$C_{99}H_{127}N_{19}O_{21}$	$C_{119}H_{151}N_{23}O_{25}$	$C_{139}H_{175}N_{27}O_{29}$
Dimensions [mm]	0.2×0.1×0.1	0.1×0.05×0.05	0.05×0.02×0.02	0.1×0.05×0.02	0.2×0.1×0.1
Color	colorless	colorless	colorless	colorless	colorless
Crystal system	triclinic	triclinic	triclinic	orthorhombic	monoclinic
Space group	$P\bar{1}$	$P\bar{1}$	$P\bar{1}$	*Pbca*	*C*2/*c*
Z (Z')	2 (4)	2 (4)	2 (2)	8 (2)	8 (1)
a [Å]	21.0120 (10)	20.5203 (8)	20.865 (4)	40.4820 (10)	38.8452 (10)
b [Å]	24.493 (2)	32.7070 (12)	21.927 (4)	39.6920 (10)	22.7274 (3)
c [Å]	29.916 (2)	34.4280 (12)	33.746 (7)	40.8340 (10)	46.2275 (18)
α [°]	111.175 (5)	66.740 (2)	73.59 (3)	90	90
β [°]	103.361 (5)	75.940 (2)	76.52 (3)	90	115.5700
γ [°]	93.590 (5)	72.402 (2)	61.90 (3)	90	90
T [K]	193 (2)	133 (2)	100 (2)	100 (2)	113 (2)
V [Å^3]	13785.8 (16)	20032.7 (13)	12973 (4)	65613(3)	36814.8 (18)
ρ [g cm^{-3}]	1.205	1.187	1.184	1.271	1.215
λ [Å]	1.54178	1.54178	0.80000	0.80000	1.54178
θ measured	6.51 < θ < 54.24	6.50 < θ < 39.97	3.46 < θ < 23.58	4.13 < θ < 30.00	6.34 < θ < 50.43
Reflns measured	30856	158533	42570	458594	112324
unique reflections	30856	24106	21957	32604	18787
GOF	1.013	1.016	1.102	1.018	1.020
R1 (all data)	0.2109	0.1720	0.2064	0.1565	0.2009
wR2 (all data)	0.5267	0.4618	0.5208	0.4864	0.5417
CCDC#	757948	757946	757944	757945	757947

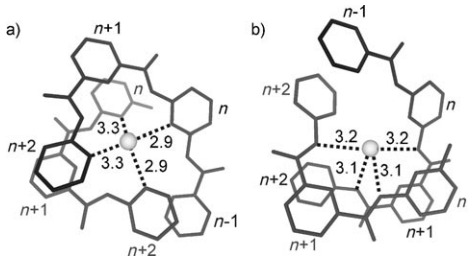

Figure 2. Top views of the stick representation of fragments of $(\mathbf{9a})_2$ in the crystalline state and potential interactions (dashed lines) between each color-coded strand of the duplex and a water molecule: a) potential hydrogen bonds between the water hydrogens and endocyclic nitrogen atoms belonging to neighboring 2,6-diaminopyridine rings; b) potential hydrogen bonds between the water oxygen atom and neighboring carboxamide hydrogens. Atomic distances are given in Angstroms. Isobutoxy side chains and hydrogen atoms have been omitted for clarity.

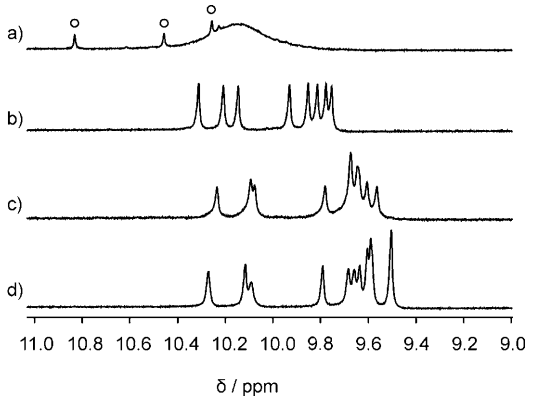

Figure 3. Part of the 400 MHz ^{1}H NMR spectra at 20 °C of 2 mM $CDCl_3$ solutions showing the amide resonances of: a) **7a**; b) **9a**; c) **11a** and d) **13a** shortly after dissolving the crystals. Signals belonging to the single helix are marked with circles.

(Figure 2). These latter interactions are not firmly established because the positions of water hydrogen atoms in the structures have not been determined experimentally. Each water molecule potentially creates bridging interactions between the two strands. However, it has not been established whether these interactions ultimately stabilize double helical architectures. Indeed, water is also bound in the channel of single helical conformers,[23] and water has been shown to promote duplex dissociation in solution.[9b]

Solution Studies in $CDCl_3$

The association of **5a**–**13a** into double helical architectures in the solid state underlines the high propensity of the pyridinecarboxamide oligomers to hybridize. However, the crystallization of **11a** and **13a** as double helices came as a surprise because of our earlier finding that K_{dim} values quickly drop upon increasing strand length, leading to a value of the order of 65 $L\,mol^{-1}$ for the 13 mer having decyloxy side chains and Cbz terminal groups.[9c] NMR studies were thus undertaken to quantify the double helix formation in solution. NMR is convenient because single helices and double helices are in slow exchange on the NMR time scale for oligomers of seven pyridine units or more and give rise to two sets of signals that can be integrated to calculate K_{dim}. Several spectroscopic features specific to either single or double helices help in the assignment of the signals. Below a certain temperature, the lower symmetry of the double helix gives rise to twice as many signals as the single helix.[9a,c] The proportion of single helix increases upon heating and dilution while intermolecular aromatic stacking within double helices results in stronger ring current effects, which causes upfield shifts of the double helix signals.

The ^{1}H NMR spectrum of heptamer **7a** in $CDCl_3$ shows that this compound is largely hybridized at 2 mM (broad signal) in this solvent but signals of the single helix are also clearly visible (Figure 3a). On the other hand, the ^{1}H NMR spectra of **9a**, **11a**, and **13a** all show a single set of sharp signals which can unambiguously be assigned to double helices based on their multiplicity. The exclusive presence of double helices is in agreement with the solid-state structures, but it suggests a very high K_{dim} for these compounds, which is in apparent contradiction with our previous finding.[9c] This discrepancy cannot be explained by the structural differences between this series of compounds and the previous one. Indeed, the replacement of *n*-decyloxy side chains by isobutoxy side chains was not expected to have any significant effect, and the replacement of the terminal benzylcarbamates by *tert*-butylcarbamates, though it may change duplex stability, can hardly give rise to an apparent enhancement of K_{dim} of over 4 orders of magnitude in the case of **13a**. Rather, we suspected that the equilibrium between single and double helices may be very slow in $CDCl_3$ for long oligomers and that either the spectra in Figure 3 or those on which we based our previous calculations,[9c] or both, may not reflect equilibrium and the actual K_{dim} value. This possibility was supported by a study of the hybridization of an 11 mer into a double helix comprised of pyridine, quinoline, and diaza-anthracene units, for which single-double helix equilibrium is so slow that the two species can be separated on silica gel chromatography and equilibrium can be reached in solution over several days at room temperature.[9j] To clarify this, we systematically investigated the association and dissociation kinetics of the double helices of **7a**, **9a**, **11a**, and **13a**.

As shown in Figure 4, the proportion of $(\mathbf{7a})_2$ drops significantly with a decrease in concentration and also an increase in temperature. However, heating and cooling cycles are followed by a rapid return to the original NMR spectra, which indicates that the equilibrium between single and double helices is fast with respect to the time required to fully acquire the NMR spectra. Thus, $K_{dim} = 31\,000\ L\,mol^{-1}$ can be reliably calculated at 20 °C for **7a**. This value is of the order of those previously reported for other pyridinecarboxamide heptamers bearing alkoxy groups (R) as side chains and terminal amine residues (82 000 $L\,mol^{-1}$ with R = methoxy)[9k] or decanoyl residues (65 000 $L\,mol^{-1}$ with R = decyloxy).[9a] Lower values were observed when the terminal group was

CHEMISTRY
AN ASIAN JOURNAL

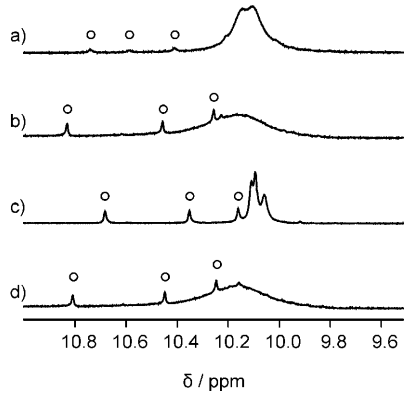

Figure 4. Part of 400 MHz ^{1}H NMR spectra in $CDCl_3$ showing the amide resonances of **7a** at different concentrations and temperatures: a) 12.8 mM at 20 °C; b) 2 mM at 20 °C; c) 2 mM at 40 °C; d) return to 2 mM at 20 °C. Spectra b), c) and d) were recorded from the same 2 mM solution at regular time intervals (30 min). Signals assigned to the single helix are marked with circles.

Cbz (1500 L mol^{-1} with R = decyloxy, 1000 L mol^{-1} with R = methoxy).[9c]

We have found that **9a** behaves differently, which is evident upon heating a solution of pure double helix, wherein signals of the single helix appear above 50 °C and remain upon cooling back to 20 °C (Figure 5). The single helix signals intensity then decreases over a couple of days but do not completely disappear. The initial spectrum at 20 °C thus appears not to reflect thermodynamic equilibrium but simply the crystal content. Furthermore, upon incubating freshly dissolved **9a** at 20 °C, the single helix signals also emerge after a couple of days without heating (not shown). The final spectra of these two experiments are identical and allow to unambiguously calculate K_{dim} to be 7×10^5 L mol^{-1} for **9a**. The nonamer thus has a propensity to form double helices about 20 times larger than the heptamer, as observed in other series, but does so at much slower association and dissociation rates. To investigate these kinetics, we prepared a sample of **9a** strongly enriched in single helix by first heating a solution in pyridine (vide infra), evaporating it, and redissolving the sample in chloroform. Equilibrium was reached within 1–2 days (Figure 6). Such slow kinetics were not observed before for other 9 mers bearing terminal amino or Cbz groups. A possible explanation is that, in the present case, the terminal Boc groups sterically hinder association and dissociation, which is in agreement with the slippage mechanism proposed for these processes.[18]

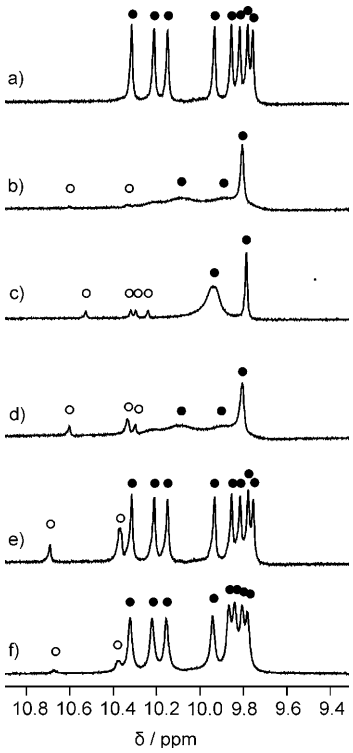

Figure 5. Part of the 400 MHz ^{1}H NMR spectra in 2 mM $CDCl_3$ solution showing amide resonances of **9a** upon changing temperature: a) 20 °C; b) 40 °C; c) 50 °C; d) 40 °C; e) 20 °C; f) 20 °C after 7 days. Spectra were recorded from the same solution at regular time intervals of 15 min per 10 °C.

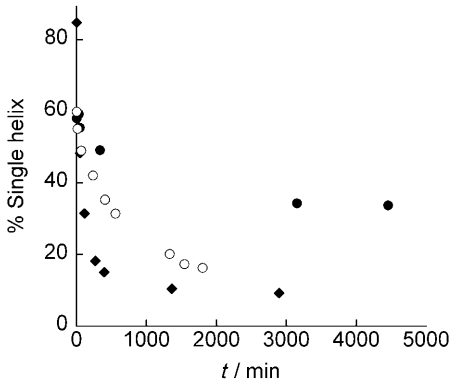

Figure 6. Time trace of duplex formation of 2 mM $CDCl_3$ solutions of **9a** (white circles) and **11a** (black circles) and of **11b** (black rhombus) after initial enrichment in single helix, as monitored by ^{1}H NMR at 20 °C.

Similar investigations were attempted with **11a** and **13a**. However, for these two longer oligomers, heating $CDCl_3$ solutions to 50 °C or incubating over 6 months in a sealed NMR tube at room temperature did not lead to any trace of single helix. This may arise either from extremely slow kinetics of duplex dissociation or from a very high K_{dim} value. To elucidate this, **11a** was treated in the same way as **9a**. A sample of **11a** was enriched in single helix by first heating a solution in pyridine (vide infra), evaporating it, and redissolving the sample in chloroform. The proportion of single helix as a function of time showed a sharp decrease (Figure 6). Equilibrium was obviously not reached after a week of incubation, and yet this shows that strand association is not kinetically inert, which suggests that the absence of change in the spectrum of freshly dissolved **11a** and **13a** reflects high thermodynamic stability (the proportion of single helices is negligible at mM concentration). Thus, K_{dim}

values for **11a** and **13a** appear to be too high to be measured by NMR in $CDCl_3$. A few attempts to measure them by UV spectroscopy also proved unsuccessful. We thus wished to investigate hybridization in a solvent less favorable to duplex formation than $CDCl_3$. DMSO was often used by us in the past for this purpose, but both **11a** and **13a** are insoluble in this solvent. In the following, we show that [D_5]pyridine proved to be a good medium to promote duplex dissociation.

Solution Studies in Pyridine

Upon dissolving **7a** and **9a** crystals (i.e., pure double helices) in [D_5]pyridine, single helices were formed at rates too fast to monitor by NMR. The final proportions allowed the calculation of K_{dim} to be 10 and 19 $L\,mol^{-1}$ for **7a** and **9a**, respectively (Figure 7). Thus this solvent causes a dramatic

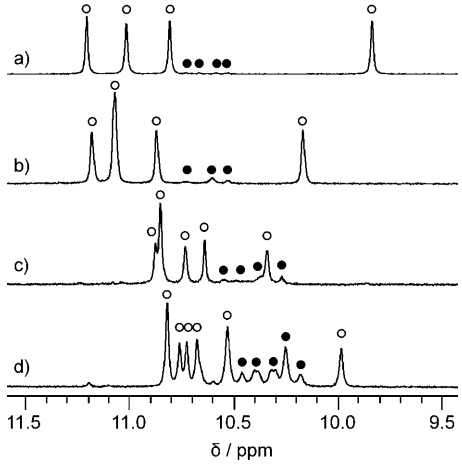

Figure 7. Part of the 300 MHz ^{1}H NMR spectra at 20 °C of 2 mM [D_5]pyridine solutions showing the amide resonances of: a) **7a**; b) **9a**; c) **11a** and d) **13a** at equilibrium. Signals belonging to the single and double helix are respectively marked with white and black circles.

decrease in double helix stability (or an increase in single helix stability), and also allows much faster strand dissociation. This effect was confirmed in the case of **11a** and **13a**. Duplexes dissociated to reach equilibrium in only one day for **11a** and 3 days for **13a** (Figure 8). That equilibrium is indeed reached could be validated through a heating and cooling cycle which led to a further increase of the proportion of single helix (heating) and a return to the equilibrium state (cooling). The time scale of strand association monitored after heat-induced dissociation was found to be the same as the time scale of strand dissociation upon dissolving crystals of double helices (not shown). From the NMR spectra K_{dim} was found to be 43 and 307 $L\,mol^{-1}$ for **11a** and **13a**, respectively. However, the kinetics could not be fitted to a simple model because the reaction is reversible. Thus, the overall trend observed in chloroform, that double helix formation is enhanced upon increasing strand length, is confirmed in [D_5]pyridine, albeit at much lower levels. It is also confirmed that rates of strand association and dissociation drop by several orders of magnitude upon increasing strand length, though at overall faster rates in [D_5]pyridine than $CDCl_3$.

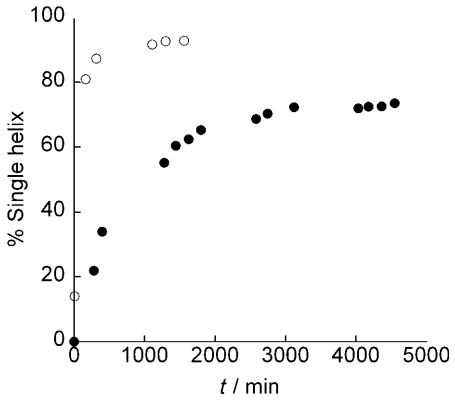

Figure 8. Time trace of duplex dissociation of 2 mM solutions of **11a** (white circles) and **13a** (black circles) in [D_5]pyridine monitored by ^{1}H NMR at 20 °C. The initial state is a freshly dissolved crystalline double helix.

The Effect of End Groups

The dimerization constants of **7a** and **9a** in $CDCl_3$ have been shown to be 3.1×10^4 $L\,mol^{-1}$ and 7×10^5 $L\,mol^{-1}$, respectively, and those of **11a** and **13a** are too high to measure, which means well above 10^6 $L\,mol^{-1}$. These values are to be compared to those we previously reported for analogues of **7a**–**13a** bearing decyloxy side chains and Cbz end groups instead of isobutoxy and Boc, which are 1500, 5200, 650, and 65 $L\,mol^{-1}$ from 7 mer to 13 mer, respectively.[9c] The discrepancy at the 7 mer and 9 mer level may be ascribed to an effect of the Boc versus Cbz end-groups, which results in K_{dim} values 20 fold (7 mer) and 130 fold (9 mer) larger in favor of Boc end groups. A possible origin of this effect is that bulky Boc end groups may have a destabilizing effect on the single helices because of steric hindrance, which facilitates their spring-like extension and thus decreases the associated enthalpy cost during hybridization.[9i] However, the discrepancy at the 11 mer and 13 mer level is far too large to simply reflect an effect of end groups which would be expected to result in a $\Delta\Delta G$ independent of strand length (i.e., a constant ratio of K_{dim} values). Instead, we suspected that our initially reported values were erroneous because they were measured away from equilibrium. The kinetics of strand dissociation for 11 mers and 13 mers are slow, and the proportions used to calculate K_{dim} may instead have reflected snapshots on the way to equilibrium.[24,25] In order to lift any doubt on this issue, we prepared **11b**, an analogue of **11a** bearing terminal Cbz groups (Scheme 1 and 2).

Crystals of **11b** were grown from a liquid–liquid diffusion of methanol into a chloroform solution. Upon dissolving this material in $CDCl_3$, an NMR spectrum very similar to that of

CHEMISTRY
AN ASIAN JOURNAL

11a (Figure S6 in the Supporting Information) was recorded. Only one species was observed and the chemical shift values and multiplicity of the signals were clearly indicative of a double helical architecture. After several days, no single helix was detected and the spectrum remained unchanged. However, upon dissolving **11b** in [D_5]pyridine, rapid dissociation occurred, which led to an almost quantitative conversion to single helix that indicated a very low K_{dim} in this solvent. After evaporation of pyridine and dissolving **11b** in $CDCl_3$, the single helix was progressively transformed almost completely into a double helix over a period of 1 day (Figure 9). This hybridization process was thus considerably more rapid than for **11a** (Figure 6).

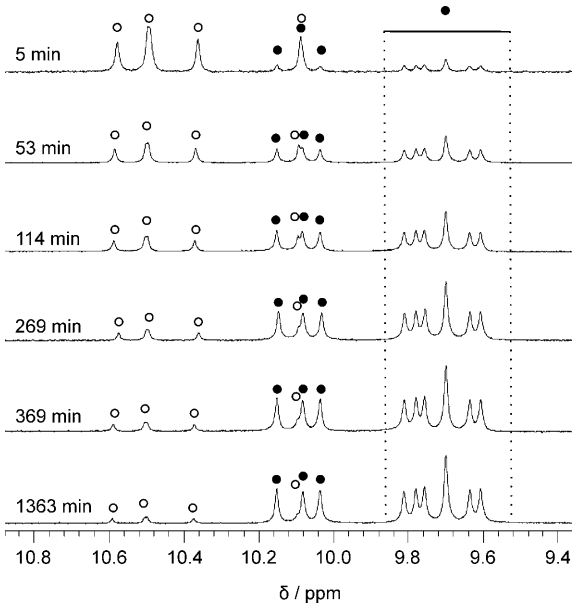

Figure 9. Part of the 300 MHz ^{1}H NMR spectra showing the formation of double helix from a 2 mM solution of Z-11 mer-Z. The selected window presents the amide resonances as a function of time. The solution was first heated in [D_5]pyridine to obtain a totally dissociated state and cooled to room temperature. Then, the spectra were recorded at 20 °C in $CDCl_3$.

Altogether, these result indicate that: (i) oligomers with Z end-groups have a propensity to hybridize one to two orders of magnitude lower that those with Boc end groups both in $CDCl_3$ and [D_5]pyridine; (ii) the K_{dim} of **11b** in $CDCl_3$ is nevertheless above 10^6 L mol^{-1}, in disagreement with that reported for an analogue of **11b** having decyloxy chains;[9c] (iii) the kinetics of association and dissociation are faster with Z-terminated oligomers, but may nevertheless take over a day for an 11 mer. It thus clearly appears that large end groups slow down kinetics and also shift equilibria in favor of double helices. Also, we conclude that our low K_{dim} value reported for a 13 mer and an 11 mer were in fact measured out of equilibrium because of the slow kinetics involved. This may have been enhanced by the decyloxy chains of the oligomers investigated at the time which might have expectedly resulted in slower kinetics than with isobutoxy chains, though without alteration in thermodynamics.

Conclusions

In summary, we have validated our assumption that isobutoxy side chains provide both high solubility and high crystallinity and have shown compelling crystallographic evidence that hybridization of pyridinecarboxamide oligomers may occur over extended strand lengths and follow a highly conserved structural motif. Solution studies have revealed that increasing strand length results in a strong increase of the propensity to hybridize in double helical structures. Increasing strand length also causes a dramatic decrease in the strand association and dissociation kinetics, where timescales range from minutes to weeks upon elongation of a heptamer to a tridecamer. These effects have been observed in $CDCl_3$ in which hybridization is favored (K_{dim} ranging from 10^4 to above 10^6 L mol^{-1}). They also persist in [D_5]pyridine where hybridization is much weaker (K_{dim} ranging from 10 to 300 L mol^{-1}) and strand association and dissociation proceeds at faster rates. This study underlines the potentially critical importance of kinetic aspects when assessing the stability of non-covalent assemblies even though of relatively small size. Indeed, for having overlooked the slow kinetics of hybridization of the longest strands, two K_{dim} values published by us were found to be erroneous.[9c]

We also observed that bulky Boc terminal groups result in a one to two orders of magnitude enhancement of K_{dim} when compared to terminal flat Cbz groups. This effect was tentatively assigned to a facilitated spring-like extension of single helices. Bulky Boc terminal groups also result in slower kinetics of strand association and dissociation than terminal Cbz groups, which is in agreement with the current proposed slippage mechanism of hybridization, in which one single helical strand proceeds within another one in a screw-like motion.

The hybridization of pyridinecarboxamide oligomers into double helices results from a subtle combination of various non independent parameters, namely, ability to extend like springs, oligomer length, and nature of side chains and of terminal groups. All of them critically influence both the thermodynamic and kinetic aspects. Combined with previous investigations, the results presented here have framed a global understanding of this complex and intriguing phenomenon and provide useful guidelines for the design of other artificial double helices.

Experimental Section

General procedure and materials. Unless specified, materials were obtained from commercial suppliers and used without further purification. NMR spectra were recorded on a Bruker-Avance 400 NB US NMR spectrometer by means of a 5 mm direct QNP 1H/X probe with gradient capabilities. Samples were not degassed. Chemical shift are reported in ppm and are calibrated against residual solvent signals of $CDCl_3$ (δ = 7.26, 77.2 ppm), [D_6]DMSO (δ = 2.50, 39.4 ppm), [d_5]pyridine (δ = 8.74, 7.58, 7.22 ppm). All coupling constants are reported in Hz. Silica gel chromatography was performed using Merck Kieselgel Si 60. Electronspray ionization (ESI) mass spectra were obtained in the positive ion mode.

Dimethyl 4-isobutyloxy-2,6-pyridine dicarboxylate 1a. Anhydrous dimethyl chelidamic ester[26] (8.3 g, 34 mmol, 1equiv) was dissolved in 60 mL of freshly distilled DMF and heated to 120 °C under a N_2 atmosphere. K_2CO_3 (14.0 g, 102 mmol, 3 equiv) was added and heating at 120 °C was continued for 1.5 h. After cooling down to 70 °C, isobutyl iodide (6.2 mL, 51 mmol, 1.5 equiv) was added and the mixture was stirred at 70 °C for 3 h. The solution was cooled to room temperature. Solid residues were filtered off. Toluene (80 mL) and water (50 mL) were added. The mixture was extracted twice with toluene (80 mL). The combined organic layers were dried with Na_2SO_4 and evaporated under vacuum to obtain the product as a white solid. Yield 8.7 g (90 %); m.p.: 76–78 °C; ^{1}H NMR (400 MHz, [D6]DMSO): $\delta = 7.73$ (2 H, s), 4.01 (2 H, d, $J = 6.0$), 3.91 (6 H, s), 2.07 (1 H, m), 1.00 ppm (6 H, d, $J = 6.4$); ^{13}C NMR ($CDCl_3$): $\delta = 166.40$, 164.50, 149.25, 113.96, 74.50, 52.56, 27.37, 18.65 ppm; ESI-MS: *m/z* (%) calcd for $C_{13}H_{17}NO_5$: 267.1; found: 268.0 $[M+H]^+$, 290.1 $[M+Na]^+$, 556.8 $[2M+Na]^+$.

4-isobutyloxy-2,6-pyridinedicarboxylic acid 1c. Diester **1a** (1.34 g, 5 mmol) was dissolved in a mixture of methanol (10 mL), 1,4-dioxane (10 mL) and water (5 mL). NaOH (0.6 g, 15 mmol) was added and the solution was stirred at 25 °C. The progress of saponification was monitored by TLC. Acetic acid (1.3 mL) was added and the resulting white precipitate was filtered off and washed thoroughly with ethyl acetate and diethyl ether. Yield 1.13 g (95 %); m.p.: 171–173 °C; ^{1}H NMR (400 MHz, [D_6]DMSO): $\delta = 7.51$ (2 h, s), 4.03 (2 H, d, $J = 6.4$ Hz), 2.08 (1 H, m), 1.01 ppm (6 H, d, $J = 6.8$); ESI-MS: *m/z* (%) cacld for $C_{11}H_{13}NO_5$: 239.1; found: 240.2 $[M+H]^+$.

4-isobutyloxy-2,6-pyridinedicarboxylic acid monomethyl ester 1d. Diester **1a** (1.34 g, 5 mmol) was dissolved in a mixture of 1,4-dioxane (24 mL) and methanol (7 mL) and the solution was cooled to 0 °C. NaOH (0.2 g, 5 mmol) was added and the solution was stirred for 2 h at 25 °C. The progress of saponification was monitored by TLC. The solution was acidified with acetic acid and poured into 100 mL water, and then extracted with CH_2Cl_2 (2 × 50 mL). The solvent was evaporated and the residue was dried under vacuum and used directly without further purification. Yield 0.91 g (72 %); m.p.: 93–95 °C; ^{1}H NMR (400 MHz, $CDCl_3$): $\delta = 7.85$ (1 h, s), 7.82 (1 H, s), 4.01 (3 H, s), 3.92 (2 H, d, $J = 6.4$), 2.16 (1 H, m), 1.05 ppm (6 H, d, $J = 6.4$); ^{13}C NMR ($CDCl_3$): $\delta = 176.78$, 164.03, 163.75, 147.99, 115.53, 114.20, 111.90, 75.19, 52.75, 27.6, 18.61 ppm; ESI-MS: *m/z* (%) cacld for $C_{12}H_{15}NO_5$: 253.1; found: 254.1 $[M+H]^+$, 528.8 $[2M+Na]^+$.

2,6-diamino-4-isobutyloxy-pyridine 1b. Dry NH_3 gas was gently bubbled into a solution of 4-isobutyloxy-2,6-pyridinedicarboxylate **1a** (3.5 g, 13.1 mmol) in methanol (45 mL) for 1 h. The resulting white precipitate of 4-isobutyloxy-2,6-pyridinedicarboxamide was filtered off, dried under vacuum and used without further purification (2.8 g, 90 %). M.p.: 190–192 °C; ^{1}H NMR (400 MHz, [D6]DMSO): $\delta = 8.83$ (2 H, s), 7.69 (2 H, s), 7.63 (2 H, s), 3.97 (2 H, d, $J = 6.0$), 2.05 (1 H, m), 0.99 ppm (6 H, d, $J = 5.6$); ESI-MS: *m/z* (%) calcd for $C_{11}H_{15}N_3O_3$: 237.1; found: 238.1 $[M+H]^+$, 260.1 $[M+Na]^+$. KOH (10 g, 178 mmol) was dissolved in water (20 mL) at 0 °C. Crushed ice (25 g) was added, followed by the slow addition of Br_2 (1.3 mL, 25.4 mmol) with continuous stirring. After 10 min, 4-isobutyloxy-2,6-pyridinedicarboxamide (2.37 g, 10 mmol) was added, followed by 1,4-dioxane (45 mL). The mixture was stirred in an ice bath for 10 min, at 25 °C for 1 h and then heated to 70 °C for 1.5 h. Acetic acid (6 mL) was added and, afer 30 min, the reaction mixture was cooled to 25 °C, and KOH (4 g) was added. The solution was extracted with dichloromethane. The organic phase was evaporated and the residue was purified by flash chromatography (SiO_2) with methanol/ethyl acetate (5:95 vol/vol) as eluent to yield 1.42 g of **1b** as a light yellow solid (78 %); m.p.: 104–106 °C; IR (Liquid layer): $\tilde{\nu} = 3435$, 3373, 3192, 2963, 2919, 2876, 1639, 1447, 1198, 1030 cm^{-1}; ^{1}H NMR (400 MHz, $CDCl_3$): $\delta =$ 5.48 (2 H, s), 4.12 (4 H, s), 3.65 (2 H, d, $J = 6$), 2.03 (1 H, m), 0.99 ppm (6 H, d, $J = 6.8$); ^{13}C NMR ($CDCl_3$): $\delta = 168.76$, 158.91, 84.67, 73.88, 28.04, 19.14 ppm; ESI-MS: *m/z* (%) calcd for $C_9H_{15}N_3O$: 181.1; found: 182.1 $[M+H]^+$.

(4-isobutyloxy-6-amino-pyridin-2-yl)-carbamic acid *tert*-butyl ester 1e. Lithium bis(trimethylsilyl)amide (1.0 M in THF, 15.8 mL, 2 equiv) was added dropwise to a solution of 4-isobutyloxy-2,6-diaminopyridine **1b** (1.43 g, 7.9 mmol, 1 equiv) in dry THF (10 mL) through a period of 15 min at 25 °C. After 10 min, a solution of di-*tert*-butyldicarbonate (1.72 g, 1 equiv) in dry THF (10 mL) was added slowly over 20 min. The reaction was allowed to proceed at 25 °C for 3 h. The solvent was removed and the residue was dissolved in CH_2Cl_2 (50 mL) and extracted with water (2 × 50 mL). The combined organic layers were evaporated and the residue was purified by column chromatography (SiO_2) with cyclohexane/ethylacetate/triethyl amine (70:25:5, vol/vol/vol) as eluent to afford **1e** as a light yellow wax (1.15 g, 52 %). IR (liquid layer): $\tilde{\nu} = 3484$, 3379, 3205, 2969, 2931, 2876, 1782, 1720, 1614, 1571, 1447, 1391, 1372, 1285, 1235, 1161, 1037 cm^{-1}; ^{1}H NMR (400 MHz, $CDCl_3$): $\delta = 6.95$ (1 H, s), 6.92 (1 H, s), (5.7, 1 H, s), 4.16 (2 H, s), 3.74 (2 H, d, $J = 6.4$ Hz), 2.04 (1 H, s), 0.99 ppm (6 H, d, $J = 6.8$ Hz); ^{13}C NMR ($CDCl_3$): $\delta = 169.24$, 168.64, 159.43, 158.8, 152.88, 152.29, 11.42, 92.05, 90.00, 89.27, 83.15, 81.09, 74.54, 28.71, 28.36, 19.59 ppm; ESI-MS: *m/z* (%) cacld for $C_{14}H_{23}N_3O_3$: 281.2; found: 281.9 $[M+H]^+$.

Cbz-momomer amine 1f. Lithium bis(trimethylsilyl)amide (LiHMDS) (1.0 M^{-1}, 11.0 mL, 11.0 mmol, 2 equiv) was added dropwise to a solution of 4-isobutyloxy-2,6-diamino-pyridine (**1b**, 1.0 g, 5.5 mmol, 1 equiv) in dry THF (10 mL) at 0 °C over a period of 15 min. After 10 min, a solution of benzyl chloroformate (0.80 mL, 7.9 mmol, 1 equiv) in dry THF (10 mL) was added over 20 min. The reaction was then allowed to proceed at room temperature for 3 h. The solvent was removed and the residue was dissolved in CH_2Cl_2 (50 mL) and extracted with water (2 × 50 mL). The organic layer was evaporated and the residue was purified by column chromatography using cyclohexane/ethyl acetate/triethyl amine (70:25:5 vol/vol/vol) as eluent to afford a light yellow wax (0.97, 56 %). ^{1}H NMR (400 MHz, $CDCl_3$): $\delta = 7.61$ (1 H, brs), 7.38–7.35 (4 H, m), 6.99 (1 H, s), 5.71 (s, 1 H), 5.21 (2 H, s), 4.24 (2 H, brs), 3.74 (2 H, d), 2.06 (1 H, m), 1.01 ppm (6 H, d); ESI-MS: *m/z* (%) calcd for $C_{17}H_{21}N_3O_3$: 315.2; found: 316.1 $[M+H]^+$).

Trimer di-Boc 3a. Diacid **1c** (434 mg, 1.82 mmol, 0.7 equiv) and thionyl chloride (10 mL) were heated to reflux for 0.5 h, under a nitrogen atmosphere. Excess thionyl chloride was removed first under reduced pressure, and then with a toluene azeotrope. The residue was dissolved in dry THF (10 mL). This solution was added dropwise to a previously prepared solution of **1e** (850 mg, 3.02 mmol, 1 equiv) in dry THF (10 mL) and diisopropylethylamine (1.08 mL, 2.5 equiv) at 25 °C. The reaction mixture was stirred at 25 °C for 12 h. The solvent was removed and the residue was purified by flash chromatography (SiO_2) with ethyl acetate/CH_2Cl_2 (5:95 vol/vol) as the eluent to yield the product (860 mg, 75 %). M.p.: 140–142 °C; IR (liquid layer): $\tilde{\nu} = 3644$, 3375, 3300, 3138, 3056, 2963, 2931, 2875, 1731, 1694, 1613, 1581, 1513, 1444, 1394, 1363, 1225, 1163, 1081, 1038 cm^{-1}; ^{1}H NMR (400 MHz, $CDCl_3$): $\delta = 10.31$ (2 H, s), 7.95 (2 H, s), 7.76 (2 H, s), 7.31 (2 H, s), 7.14 (2 H, S), 3.95 (2 H, d, $J = 5.6$), 3.86 (4 H, d, $J = 4.8$), 2.13 (3 H, m), 1.52 (18 H, s), 1.05 ppm (18 H, d, $J = 6.4$); ^{13}C NMR ($CDCl_3$): $\delta = 168.96$, 168.20, 161.56, 152.13, 151.45, 150.45, 150.13, 111.80, 95.98, 95.00, 80.88, 75.30, 74.48, 30.26, 29.65, 28.14, 27.92, 19.15 ppm; ESI-MS: *m/z* (%) calcd for $C_{39}H_{55}N_7O_9$: 765.4; found: 766.2 $[M+H]^+$.

Trimer diamine 3b. Trimer di-Boc **3a** (850 mg, 1.11 mmol) was dissolved in CH_2Cl_2 (5 mL) and TFA (2 mL) was added to the solution. After stirring for 2 h, the reaction mixture was washed with aqueous $NaHCO_3$ solution and extracted with chloroform (2 × 50 mL). The solvent was evaporated to yield the product as a white solid (621.5 mg, 99 %). M.p.: 114–116 °C; IR (liquid layer): $\tilde{\nu} = 3370$, 3352, 2963, 2932, 2876, 1684, 1616, 1350, 1450, 1338, 1245, 1233, 1172, 1036 cm^{-1}; ^{1}H NMR (400 MHz, $CDCl_3$): $\delta = 10.23$ (2 H, s), 7.94 (2 H, s), 7.52 (2 H, s), 5.84 (2 H, s), 4.43 (4 H, S), 3.95 (2 H, d, $J = 4.4$), 3.81 (4 H, d, $J = 5.6$), 2.13 (3 H, m), 1.03 ppm (18 H, d, $J = 4.8$); ^{13}C NMR ($CDCl_3$): $\delta = 168.88$, 168.45, 158.53, 150.38, 111.67, 91.85, 90.23, 75.30, 74.31, 28.09, 19.16 ppm; ESI-MS: *m/z* (%) calcd for $C_{29}H_{39}N_7O_5$: 565.3; found: 566.36 $[M+H]^+$.

Dimer Boc-ester 2a. Monoacid **1d** (404 mg, 1.6 mmol, 1.2 equiv) and thionyl chloride (10 mL) were heated to reflux for 0.5 h under a nitrogen atmosphere. The excess thionyl chloride was removed first under reduced pressure and then with a toluene azeotrope. The residue was dissolved in dry THF (10 mL). This solution was added dropwise to a previously prepared solution of monoamine **1e** (374 mg, 1.33 mmol, 1 equiv) in dry THF (5 mL) and diisopropylethylamine (1.3 mL) at room temperature. The mixture was stirred at ambient temperature for 12 h. The solvent

was removed and the residue was purified by flash chromatography (SiO_2) with cyclohexane/ethyl acetate (2:1 vol/vol) as the eluent to yield the product (520 mg 81%). M.p.: 134–136°C; IR (liquid layer): $\tilde{\nu}$=3375, 2963, 2938, 2875, 1725, 1713, 1700, 1600, 1538, 1506, 1444, 1394, 1388, 1363, 1331, 1225, 1156, 1113, 1088, 1038 cm^{-1}; ^1H NMR (400 MHz, $CDCl_3$): δ=10.16 (1H, s), 7.92 (1H, s), 7.76 (1H, s), 7.66 (1H, s), 7.3 (1H, s), 7.03 (1H, s), 4.02 (3H, s), 3.92 (2H, d, J=6.4), 3.85 (2H, d, J=6.8), 2.13 (2H, m), 1.52 (9H, s), 1.04 ppm (12H, d, J=4.0); ^{13}C NMR ($CDCl_3$): δ=169.31, 168.02, 165.33, 162.06, 152.51, 150.40, 148.59, 115.22, 111.32, 95.83, 95.02, 81.27, 75.57, 74.84, 53.27, 28.55, 1048 ppm; ESI-MS: m/z (%) calcd for $C_{26}H_{36}N_4O_7$: 516.3; found: 517.0 $[M+H]^+$.

Dimer Boc-acid 2b. Sodium hydroxide (80 mg, 2 equiv) was added to a solution of dimer ester **2a** (516 mg, 1 mmol) in 1,4-dioxane (25 mL) and water (2 mL) at room temperature, and the resulting solution was stirred for 2 h, then acidified with acetic acid. CH_2Cl_2 (40 mL) was then added to the reaction mixture. The organic phase was washed with water, then dried with $MgSO_4$ and filtered. The solvent was removed and the residue was purified by flash chromatography (SiO_2) with cyclohexane/ethyl acetate (from 2:1 to 1:1 vol/vol) as the eluent to give the product (452 mg, 90%). M.p.: 160–162°C; IR (liquid layer): $\tilde{\nu}$=3250, 3133, 2967, 2930, 2874, 1724, 1706, 1693, 1583, 1447, 1392, 1361, 1331, 1238, 1158, 1085, 1035 cm^{-1}; ^1H NMR (400 MHz, $CDCl_3$): δ=10.56 (1H, s), 8.11 (1H, s), 7.98 (1H, s), 7.93 (1H, s), 7.73 (1H, s), 7.66 (1H, s), 3.96 (2H, d, J=4.4), 3.87 (2H, d, J=6.8), 2.16 (2H, m), 1.48 (9H, s), 1.05 ppm (12H, d, J=4.0); ^{13}C NMR ($CDCl_3$): δ=170.35, 168.23, 162.87, 152.56, 151.30, 149.87, 114.80, 112.13, 96.25, 95.20, 81.69, 75.57, 75.25, 28.65, 19.56 ppm; ESI-MS: m/z (%) calcd for $C_{25}H_{34}N_4O_7$: 502.2; found: 503.19 $[M+H]^+$.

Pentamer di-Boc 5a. 1-Chloro-*N*,*N*,2-trimethylpropenylamine[20] (1.2 mmol, 0.1 mL, 6 equiv) was added to dimer acid **2b** (251 mg, 0.5 mmol, 2.5 equiv) dissolved in dry CH_2Cl_2 (2 mL) under a nitrogen atmosphere. The mixture was stirred for 12 h at 25°C. Excess chloroenamine was removed under reduced pressure. The residue obtained was dissolved in dry CH_2Cl_2 (2 mL) and added dropwise to a previously prepared solution of monomer di-amine **1b** (36 mg, 0.2 mmol, 1 equiv) in dry CH_2Cl_2 (2 mL) and diisopropylethylamine (1.3 mL) at 25°C. The mixture was stirred at ambient temperature for 12 h. The solvent was removed and the residue was purified by flash chromatography (SiO_2) with ethyl acetate/cyclohexane (5:95 vol/vol) as the eluent to yield the product (218 mg, 95%). M.p.: 116–118°C; ^1H NMR (400 MHz, $CDCl_3$): δ=10.35 (2H, s), 10.26 (2H, s), 7.76 (2H, s), 7.68 (2H, s), 7.40 (2H, s), 7.07 (2H, s), 6.66 (4H, s), 3.95 (6H, d, J=6.8), 3.70 (2H br), 3.53 (2H, br), 2.17 (5H, m), 1.15 (18H, s), 1.11 ppm (30H, d, J=6.4); ^{13}C NMR ($CDCl_3$): δ=168.26, 167.75, 161.30, 161.06, 151.20, 150.80, 150.41, 149.99, 111.44, 110.97, 97.43, 95.63, 93.95, 80.45, 75.3, 74.08, 48.53, 39.11, 28.23, 27.76, 20.58, 19.16, 19.08 ppm; ESI-MS: m/z (%) calcd for $C_{59}H_{79}N_{11}O_{13}$: 1149.6; found: 1150.4 $[M+H]^+$.

Dimer Cbz Ester 2c. Under a nitrogen atmosphere, 4-isobutyloxy-2,6-pyridinedicarboxylic acid monomethyl ester (**1d**, 471 mg, 1.8 mmol, 1.2 equiv) was suspended in toluene (10 mL). Oxalyl chloride (0.5 mL, 4.1 mmol) and two drops of DMF were added to the suspension. The reaction mixture was stirred at room temperature for 2 h, and then excess oxalyl chloride and toluene were removed under reduced pressure. The residue was dissolved in dry THF (10 mL) and was added dropwise to a previously prepared solution of **1f** (315 mg, 1.0 mmol, 1 equiv) in dry THF (5 mL) and *N*,*N*-diisopropylethylamine (0.4 mL) at room temperature. The mixture was stirred at ambient temperature for 12 h. The solvent was removed and the residue was purified by silica gel chromatography, with cyclohexane/ethyl acetate (2:1 vol/vol) as eluent to yield the product (570 mg, 98%). ^1H NMR (400 MHz, $CDCl_3$): δ=10.20 (1H, s), 7.92 (1H, d), 7.36 (5H, m), 5.24 (2H, s), 4.04 (2H, s), 3.94 (2H, d), 3.88 (2H, d), 2.16 (2H, m), 1.06 ppm (12H, m); ESI-MS: m/z (%) calcd for $C_{29}H_{34}N_4O_7$: 550.2; found: 551.2 $[M+H]^+$.

Dimer Cbz acid 2d. To a solution of dimer ester **2c** (220 mg, 0.40 mmol) in 1,4-dioxane (15 mL) and water (2 mL) at room temperature, sodium hydroxide (40 mg, 1.0 mmol, 2.5 equiv) was added and the resulting solution was stirred for 2 h, and then acidified with acetic acid, followed by the addition of CH_2Cl_2 (40 mL). The organic layer was washed with water, then dried with $MgSO_4$ and filtered. The solvent was removed and the residue was purified by silica gel chromatography with CH_2Cl_2/EtOAc (1:5 vol/vol) containing 1% AcOH as eluent, to yield the product as a white solid (190 mg, yield: 88%). ^1H NMR (400 MHz, $CDCl_3$): δ=10.55 (1H, s), 7.99 (1H, s), 7.90 (2H, d, J=2.8 Hz), 7.76 (1H, s), 7.45–7.37 (5H, m), 5.27(2H, s), 3.94 (2H, d, J=8.8 Hz), 3.88 (2H, d, J=8.8 Hz), 2.16 (2H, m), 1.06 ppm (12H, m); ESI-MS: m/z (%) calcd for $C_{28}H_{32}N_4O_7$: 536.2; found: 537.3 $[M+H]^+$.

Pentamer diamine 5b. TFA (2 mL) was added to pentamer di-Boc **5a** (180 mg, 0.16 mmol) dissolved in CH_2Cl_2 (2 mL). After stirring for 2 h, the reaction mixture was washed with saturated aqueous $NaHCO_3$ solution and extracted with chloroform (2×50 mL). The solvent was evaporated to yield the product as a white solid (146 mg, 98%). M.p.: 172–174°C; ^1H NMR (400 MHz, $CDCl_3$): δ=10.61 (2H, s), 10.42 (2H, s), 7.88 (2H, s), 7.85 (2H, s), 7.58 (2H, s), 7.08 (2H, s), 5.31 (2H, s), 4.28 (4H, br), 3.99 (6H, d, J=5.6), 3.82 (2H br), 3.6 (2H, br), 2.17 (5H, m), 1.04 ppm (30H, d, J=6.0); ^{13}C NMR (CDCl3): δ=168.34, 167.98, 162.06, 161.80, 158.08, 150.84, 150.37, 111.52, 111.22, 98.02, 90.24, 89.76, 89.72, 75.55, 74.28, 28.39, 28.35, 19.47, 19.40 ppm; ESI-MS: m/z (%) calcd for $C_{49}H_{63}N_{11}O_9$: 949.5; found: 950 [M+H]+.

Heptamer di-Boc 7a was prepared from dimer acid **2b** (425 mg, 0.85 mmol) and trimer diamine **3a** (192 mg, 0.34 mmol) using the same procedure as for **5a**. Yield 506 mg (98%); m.p.: 124–126°C; IR (liquid layer): $\tilde{\nu}$=3391, 3336, 3317, 2967, 2936, 2911, 2887, 1687, 1724, 1737, 1613, 1583, 1527, 1509, 1490, 1441, 1386, 1324, 1171, 1152, 1041 cm^{-1}; ^1H NMR (400 MHz, [D_6]DMSO): δ=10.92 (2H, s), 10.49 (2H, s), 10.19 (2H, s), 9.31 (2H, s), 7.96 (2H, s), 7.77 (2H, s), 7.73 (2H, s), 7.50 (2H, s), 7.37 (2H, s), 7.19 (2H, s), 6.96 (2H, s), 4.11 (6H, d, J=4.4), 3.88 (4H, d, J=5.6), 3.84 (4H, d, J=5.2), 2.15 (7H. m), 1.32 (18H, s), 1.11 ppm (42H, br); ^{13}C NMR ($CDCl_3$): δ=168.17, 167.70, 167.57, 161.02, 150.98, 150.39, 150.09, 149.62, 149.41, 111.56, 111.03, 96.28, 95.04, 93.94, 80.41, 75.15, 73.96, 28.14, 27.97, 27.68, 19.15 ppm; ESI-MS: m/z (%) calcd for $C_{79}H_{103}N_{15}O_{17}$: 1533.8; found: 1534.2 [M+H]+.

Heptamer diamine 7b was prepared from heptamer di-Boc **7a** (450 mg, 0.29 mmol) using the same procedure as for **5b**. Yield 382 mg (99%); m.p.: 180–182°C; IR (liquid layer): $\tilde{\nu}$=3308, 3284, 2969, 2932, 2876, 1690, 1610, 1585, 1573, 1530, 1473, 1425, 1447, 1425, 1431, 1345, 1332, 1289, 1215, 1172, 1166, 1036 cm^{-1}; ^1H NMR (400 MHz, [D_6]DMSO): δ=11.38 (2H, s) 10.74 (2H, s), 10.30 (2H, s), 7.88 (4H, s), 7.71 (2H, s), 7.64 (2H, s), 7.56 (2H, s), 6.76 (2H, s), 5.61 (2H, s), 5.40 (4H, s), 4.08 (2H, d, J=6.4), 4.04 (4H, d, J=6.4), 3.91 (4H, d, J=6.4), 3.70 (4H, d, J=6.4), 2.14 (7H, m), 1.08 ppm (42H, br); ^{13}C NMR ($CDCl_3$): δ=168.13, 167.69, 161.65, 157.72, 150.67, 150.06, 111.34, 96.78, 91.88, 89. 55, 75.38, 74.07, 29.97, 28.46, 19.38 ppm; ESI-MS: m/z (%) calcd for $C_{69}H_{87}N_{15}O_{13}$: 1333.7; found: 1334.32 $[M+H]^+$.

Nonamer di-Boc 9a was prepared from dimer acid **2b** (140 mg, 0.28 mmol, 2.5 equiv) and pentamer diamine **5b** (107 mg, 0.11 mmol, 1 equiv) using the same procedure as for **5a**. Yield 152 mg (72%); m.p.: 138–140°C; ^1H NMR (400 MHz, [D_6]DMSO, at 101°C): δ=10.17 (2H, s), 10.02 (2H, s), 9.94 (2H, s), 9.85 (2H, s), 7.93 (2H, s), 7.81 (2H, s), 7.48 (2H, s), 7.37 (4H, s), 7,24 (2H, s), 6.86 (2H, br), 4.12 (8H, d, J=5.6), 3.97 (3H, br), 3.81 (3H, br), 2.24 (18H, s), 1.15 ppm (54H, d, J=5.0 Hz); ^{13}C NMR ($CDCl_3$): δ=168.17, 167.78, 167.38, 161.28, 160.87, 150.76, 150.20, 149.30, 117.03, 111.87, 110.37, 97.29, 94.81, 88.06, 84.03, 82.38, 81.96, 75.03, 73.89, 65.98, 29.66, 28.12, 27.6, 19.15, 19.04 ppm; ESI-MS: m/z (%) calcd for $C_{99}H_{127}N_{19}O_{21}$: 1917.9; found: 1919 $[2M++2H]^{2+}$, 1940 $[M+Na]^+$ and 1956 $[M+K]^+$.

Nonamer diamine 9b was prepared from **9a** (120 mg, 0.06 mmol) using the same procedure as for **5b**. Yield 99.5 mg (98%); m.p.: 190–192°C; ^1H NMR (400 MHz, [D6]DMSO, 62°C): δ=10.61 (2H, s), 10.39 (2H, s), 10.25 (2H, s), 9.73 (2H, s), 8.25 (2H, s), 7.77 (2H, s), 7.48 (2H, s), 7.42 (4H, s), 7.36 (2H, s), 6.84 (2H, br), 5.43 (2H, s), 5.06 (2H, s), 4.09 (8H, d, J=5.6), 3.95 (3H br), 3.87 (3H, br), 1.14 ppm (54H, d, J=5.0); ^{13}C NMR ($CDCl_3$): δ=167.93, 167.25, 161.49, 160.68, 157.34, 149.78, 149.47, 149.02, 11.93, 111.20, 110.63, 97.39, 96.93, 96.87, 95.99, 95.67, 91.27, 89.05, 75.04, 73.34, 48.94, 28.09, 28.03, 19.12, 19.07 ppm; ESI-MS: m/z (%) calcd for $C_{89}H_{111}N_{19}O_{17}$: 1717.8; found: 1719 $[2M+2H]^{2+}$.

Undecamer di-Boc 11a was prepared from dimer acid **2b** (329 mg, 0.66 mmol, 2.5 equiv) and heptamer diamine **7b** (350 mg, 0.26 mmol,

1 equiv) using the same procedure as for **5a**. Yield 414 mg (70%); m.p.: 146–148 °C; ^{1}H NMR (400 MHz, [D$_6$]DMSO, 101 °C): δ = 10.23 (2H, s), 9.97 (2H, s), 9.78 (2H, s), 9.65 (2H, s), 9.35 (2H, s), 8.13 (2H, s), 8.01 (2H, s), 7.83 (2H, s), 7.69 (4H, s), 7.39 (2H, s), 7.30 (2H, br), 7.03 (2H, br), 6.98 (2H, s), 6.76 (2H, s) 4.08 (12H, d, J = 9.6), 3.92 (10H, d, J = 11.6), 3.72 (3H, br), 2.23 (11H, m), 1.24 (18H, s), 1.15 ppm (66H, d, J = 5.0); ^{13}C NMR ($CDCl_3$): 168.12, 167.88, 167.35, 161.21, 160.84, 160.46, 151.01, 150.43, 149.71, 149.09, 148.47, 124.58, 112.50, 111.64, 110.48, 109.98, 102.04, 97.26, 95.78, 95.03, 93.38, 80.56, 89.96, 74.93, 73.75, 28.18, 27.99, 27.53, 27.51, 1938, 18.99 ppm; ESI-MS: m/z (%) calcd for $C_{119}H_{151}N_{23}O_{25}$: 2301; found: 2303 $[2M+2H]^{2+}$.

Undecamer bis-Cbz 11b was prepared from dimer acid **2d** (182 mg, 0.34 mmol, 2.5 equiv) and heptamer diamine **7b** (181 mg, 0.14 mmol, 1 equiv) using the same procedure as for **5a**. Yield: 249 mg (75%). ^{1}H NMR (400 MHz, $CDCl_3$): δ = 10.09 (1H, s), 10.04 (1H, s), 9.91 (1H, s), 9.77 (3H, m, br), 9.70 (1H, s), 9.68 (1H,s), 9.63 (1H, s), 9.58 (1H, s), 7.62 (1H, d), 7.54 (3H, m), 7.51 (1H, d), 7.46 (1H, d), 7.43 (1H,d), 7.40 (1H, d), 7.33 (3H, m), 7.16–7.11 (5H, m), 6.96–6.89 (5H, m), 6.76 (1H, s), 6.66 (1H, s), 6.61–6.56 (3H, m), 6.51 (1H, s), 6.30 (3H, s, br.), 6.20 (1H, s), 6.12 (1H, s), 4.98 (2H, t, J = 12.6 Hz), 4.48 (1H, d, J = 12.3 Hz), 4.24 (1H, d, J = 12.3 Hz), 4.07–3.77 (11H, m), 3.50–3.38 (11H, m), 2.27–1.87 (11H, m), 1.19–0.89 ppm (66H, m); ESI-MS: m/z (%) calcd for $C_{125}H_{147}N_{23}O_{25}$: 2370.09; found: 2371.1 $[M+H]^+$.

Tridecamer di-Boc 13a was prepared from dimer acid **2b** (60 mg, 0.12 mmol, 2.5 equiv) and nonamer diamine **9b** (80 mg, 0.047 mmol, 1 equiv) using the same procedure as for **5a**. Yield 102 mg (81%); m.p.: 152–154 °C; ^{1}H NMR (400 MHz, [D6]DMSO, 75 °C): δ = 10.00 (2H, s), 9.88 (4H, s), 9.76 (2H, s), 9.70 (2H, s), 9.53 (4H, s), 8.14 (2H, s) 7.72 (2H, s), 7.67 (2H, s), 7.31 (12H, br), 7.10 (2H, s), 6.99 (4H, s), 6.72 (2H, s), 5.68 (2H,s), 4.09 (14H, d, J = 5.6), 3.85 (12H, d, J = 3.4), 2.24 (13H, m), 1.24 (18H, s), 1.16 ppm (78H, d, J = 5.0); ^{13}C NMR ($CDCl_3$): δ = 167.77, 166.83, 162.83, 160.43, 160.05, 154.88, 154.48, 153.79, 149.89, 149.29, 148.71, 145.19, 112.17, 95.35, 94.51, 94.35, 88.42, 74.59, 73.36, 27.83, 27.25, 27.20, 18.68 ppm; ESI-MS: m/z (%) calcd for $C_{139}H_{175}N_{27}O_{29}$: 2686.3; found: 2687.0 $[2M+2H]^{2+}$ (Calcd for)..

X-ray crystallography. Single crystals of **5a**, **7a**, and **13a** were mounted on a Rigaku R-Axis Rapid diffractometer equipped with a MM07 microfocus rotating anode generator (monochromatized $Cu_{k\alpha}$ radiation, 1.54178 Å). The data collection, unit cell refinement and data reduction were performed by using the CrystalClear software package. The position of non-H atoms were determined by the program SHELXD and refined with SHELXH. The position of the H atoms were deduced from coordinates of the non-H atoms and confirmed by Fourrier synthesis. H atoms were included for structure factor calculations but not refined. Single crystals of **9a** and **11a** were measured on Synchrotron beam line ID 29 (ESRF, Grenoble). Data processing was performed using the same softwares as for other crystals. Details of crystallographic data can be found in the Supporting Information.

Acknowledgements

This work was supported by the French Ministry of Research (predoctoral fellowship to B.B. and postdoctoral fellowship to D.H.) and by an ANR grant (project no. NT05-3_44880). We warmly acknowledge Christoph Mueller-Dieckmann for beamtime and help during data collection on ID29 Beamline at ESRF.

[1] a) *Principles of Nucleic Acid Structure* (Ed.: Stephen Neidle), Elsevier **2008**; b) D. H. Turner, *Curr. Opin. Struct. Biol.* **1996**, *6*, 299; c) N. Sugimoto, S. Nakano, M. Yoneyama, K. Honda, *Nucl. Acids Res.* **1993**, *24*, 4501.

[2] a) K. Beck, B. Brodsky, *J. Struct. Biol.* **1998**, *122*, 17; b) G. Auerbach, F. Gaill, R. Jaenicke, T. Schulthess, R. Timpl, J. Engel, *Matrix Biol.* **1995**, *14*, 589; c) R. Berisio, A. De Simone, A. Ruggiero, R. Improta, L. Vitagliano, *J. Pept. Sci.* **2009**, *15*, 131; d) A. V. Persikov, J. A. M. Ramshow, A. Kirkpatrick, B. Brodsky, *Biochemistry* **2005**, *44*, 1414; e) R. Improta, R. Berisio, L. Vitagliano, *Protein Sci.* **2008**, *17*, 955.

[3] S. Janaswamy, R. Chandrasekaran, *Carbohydr. Res.* **2001**, *335*, 181.

[4] F. H. C. Crick, *Nature* **1952**, *170*, 882; R. D. B. Fraser, T. P. Macrae, D. A. D. Parryl, E. Suzuki, *Proc. Natl. Acad. Sci. USA* **1986**, *83*, 1179.

[5] D. A. Langs, *Science* **1988**, *241*, 188; B. M. Burkhart, R. M. Gassman, D. A. Langs, W. A. Pangborn, W. L. Duax, V. Pletnev, *Biopolymers* **1999**, *51*, 129.

[6] D. Haldar, C. Schmuck, *Chem. Soc. Rev.* **2009**, *38*, 363.

[7] Selected examples: B. Hasenknopf, J.-M. Lehn, G. Baum, D. Fenske, *Proc. Natl. Acad. Sci. USA* **1996**, *93*, 1397; C. R. Woods, M. Benaglia, F. Cozzi, J. S. Siegel, *Angew. Chem.* **1996**, *108*, 1977; *Angew. Chem. Int. Ed. Engl.* **1996**, *35*, 1830; A. Orita, T. Nakano, D. L. An, K. Tanikawa, K. Wakamatsu, J. Otera, *J. Am. Chem. Soc.* **2004**, *126*, 10389; H. Katagiri, T. Miyagawa, Y. Furusho, E. Yashima, *Angew. Chem.* **2006**, *118*, 1773; *Angew. Chem. Int. Ed.* **2006**, *45*, 1741; A. Marquis, V. Smith, J. Harrowfield, J.-M. Lehn, H. Herschbach, R. Sanvito, E. Leise-Wagner, A. V. Dorsselaer, *Chem. Eur. J.* **2006**, *12*, 5632.

[8] C. J. Leumann, *Bioorg. Med. Chem.* **2002**, *10*, 841; P. E. Nielsen, M. Egholm, R. H. Berg, O. Buchardt, *Science* **1991**, *254*, 1497; P. E. Nielsen, *Acc. Chem. Res.* **1999**, *32*, 624.

[9] a) V. Berl, I. Huc, R. Khoury, M. J. Krische, J.-M. Lehn, *Nature* **2000**, *407*, 720; b) V. Berl, I. Huc, R. Khoury, J.-M. Lehn, *Chem. Eur. J.* **2001**, *7*, 2810; c) H. Jiang, V. Maurizot, I. Huc, *Tetrahedron* **2004**, *60*, 10029; d) C. Dolain, C. Zhan, J.-M. Léger, I. Huc, *J. Am. Chem. Soc.* **2005**, *127*, 2400; e) C. Zhan, J.-M. Léger, I. Huc, *Angew. Chem.* **2006**, *118*, 4741; *Angew. Chem. Int. Ed.* **2006**, *45*, 4625; f) D. Haldar, H. Jiang, J.-M. Léger, I. Huc, *Angew. Chem.* **2006**, *118*, 5609; *Angew. Chem. Int. Ed.* **2006**, *45*, 5483; g) Q. Gan, C. Bao, B. Kauffmann, A. Grélard, J. Xiang, S. Liu, I. Huc, H. Jiang, *Angew. Chem.* **2008**, *120*, 1739; *Angew. Chem. Int. Ed.* **2008**, *47*, 1715; h) E. Berni, B. Kauffmann, C. Bao, J. Lefeuvre, D. Bassani, I. Huc, *Chem. Eur. J.* **2007**, *13*, 8463; i) E. Berni, J. Garric, C. Lamit, B. Kauffmann, J.-M. Léger, I. Huc, *Chem. Commun.* **2008**, 1968; j) D. Haldar, H. Jiang, J.-M. Léger, I. Huc, *Tetrahedron* **2007**, *63*, 6322; k) Q. Gan, F. Li, G. Li, B. Kauffmann, J. Xiang, I. Huc, H. Jiang, *Chem. Commun.* **2010**, *46*, 297.

[10] a) B. Di Blasio, E. Benedetti, V. Pavone, C. Pedone, *Biopolymers* **1989**, *28*, 203; b) G. Bunkóczi, L. Vértesy, G. M. Sheldrick, *Angew. Chem.* **2005**, *117*, 1364; *Angew. Chem. Int. Ed.* **2005**, *44*, 1340.

[11] a) H. Goto, H. Katagiri, Y. Furusho, E. Yashima, *J. Am. Chem. Soc.* **2006**, *128*, 7176; b) H. Goto, Y. Furusho, E. Yashima, *J. Am. Chem. Soc.* **2007**, *129*, 109; c) H. Goto, Y. Furusho, E. Yashima, *J. Am. Chem. Soc.* **2007**, *129*, 9168; d) H. Goto, Y. Furusho, K. Miwa, E. Yashima, *J. Am. Chem. Soc.* **2009**, *131*, 471.

[12] a) H. Sugiura, Y. Nigorikawa, Y. Saiki, K. Nakamura, M. Yamaguchi, *J. Am. Chem. Soc.* **2004**, *126*, 14858; b) H. Sugiura, M. Yamaguchi, *Chem. Lett.* **2007**, *36*, 58; c) H. Sugiura, R. Amemiya, M. Yamaguchi, *Chem. Asian J.* **2008**, *3*, 244; d) R. Amemiya, N. Saito, M. Yamaguchi, *J. Org. Chem.* **2008**, *73*, 7137.

[13] a) Y. Tanaka, H. Katagiri, Y. Furusho, E. Yashima, *Angew. Chem.* **2005**, *117*, 3935; *Angew. Chem. Int. Ed.* **2005**, *44*, 3867; b) H. Ito, Y. Furusho, T. Hasegawa, E. Yashima, *J. Am. Chem. Soc.* **2008**, *130*, 14008; c) H. Ito, Y. Furusho, T. Hasegawa, E. Yashima, *J. Am. Chem. Soc.* **2008**, *130*, 14008; d) T. Maeda, Y. Furusho, S.-I. Sakurai, J. Kumaki, K. Okoshi, E. Yashima, *J. Am. Chem. Soc.* **2008**, *130*, 7938.

[14] J. Li, J. A. Wisner, M. C. Jennings, *Org. Lett.* **2007**, *9*, 3267.

[15] T. K. Chakraborty, D. Koley, R. Ravi, A. C. Kunwar, *Org. Biomol. Chem.* **2007**, *5*, 3713.

[16] H. Gong, M. J. Krische, *J. Am. Chem. Soc.* **2005**, *127*, 1719; J. Zhu, J.-B. Lin, Y.-X. Xu, X.-B. Shao, X.-K. Jiang, Z.-T. Li, *J. Am. Chem. Soc.* **2006**, *128*, 12307; M. Li, K. Yamato, J. S. Ferguson, B. Gong, *J. Am. Chem. Soc.* **2006**, *128*, 12628; Y. Yang, J.-F. Xiang, M. Xue, H.-Y. Hu, C.-F. Chen, *Org. Biomol. Chem.* **2008**, *6*, 4198.

[17] E. A. Archer, M. J. Krische, *J. Am. Chem. Soc.* **2002**, *124*, 5074.

[18] A. Acocella, A. Venturini, F. J. Zerbetto, *J. Am. Chem. Soc.* **2004**, *126*, 2362.
[19] H. Jiang, J.-M. Léger, I. Huc, *J. Am. Chem. Soc.* **2003**, *125*, 3448.
[20] a) N. Delsuc, J.-M. Léger, S. Massip, I. Huc, *Angew. Chem.* **2007**, *119*, 218; *Angew. Chem. Int. Ed.* **2007**, *46*, 214; b) D. Sánchez-García, B. Kauffmann, T. Kawanami, H. Ihara, M. Takafuji, M.-H. Delville, I. Huc, *J. Am. Chem. Soc.* **2009**, *131*, 8642.
[21] L. Ghosez, B. Haveaux, H. G. Viehe, *Angew. Chem.* **1969**, *81*, 468; *Angew. Chem. Int. Ed. Engl.* **1969**, *8*, 454.
[22] A. Zhang, J. S. Ferguson, K. Yamato, C. Zheng, B. Gong, *Org. Lett.* **2006**, *8*, 5117.
[23] a) V. Berl, I. Huc, R. Khoury, J.-M. Lehn, *Chem. Eur. J.* **2001**, *7*, 2798; b) I. Huc, V. Maurizot, H. Gornitzka, J.-M. Léger, *Chem. Commun.* **2002**, 578.
[24] The compounds described in reference [9c] are not crystalline. Crystallization did not drive the equilibrium towards a fully hybridized or fully dissociated state. The proportions of single and double helices were probably those arising from chromatographic separation.
[25] We believe it is reasonable to assume that changing decyloxy side chains for isobutoxy side chains has no effect as far as K_{dim} values are concerned. However, these side chains may result in different association and dissociation rates, the bulkier decyloxy presumably resulting in slower kinetics.
[26] R. Chênevert, M. Dickman, *J. Org. Chem.* **1996**, *61*, 3332–3341.

Received: December 14, 2009
Published online: April 7, 2010

